Using response surface methodology (RSM) for optimizing turbidity removal by electrocoagulation/electro-flotation in an internal loop airlift reactor

T. Ntambwe Kambuyi, F. Eddaqaq, A. Driouich, B. Bejjany, B. Lekhlif, H. Mellouk, K. Digua and A. Dani

ABSTRACT

Response surface methodology (RSM) is used to optimize the electrocoagulation/electro-flotation process applied for the removal of turbidity from surface water in an internal loop airlift reactor. Two flat aluminium electrodes are used in monopolar arrangement for the production of coagulants. The central composite design is used as a second-order mathematical model. The model describes the change of the measured responses of turbidity removal efficiency and energy consumption according to the initial conductivity (X_1), applied voltage (X_2), treatment time (X_3) and inter-electrode distance (X_4). The evaluation of the model fit quality is done by analysis of variance (ANOVA). Fisher's F-test is used to provide information about the linear, interaction and quadratic effects of factors. Multicriteria methodology, mainly the desirability function (D), is used to determine optimal conditions. The results show that, for a maximal desirability function $D = 0.79$, optimal conditions estimated are $X_1 = 1{,}487$ μS/cm, $X_2 = 5$ V, $X_3 = 6.5$ min, $X_4 = 14$ mm. The corresponding turbidity removal rate and energy consumption are 84.15% and 0.215 kWh/m^3 respectively. A confirmation study is then carried out at laboratory scale using the optimal conditions estimated. The results show a turbidity removal rate of 72.05% and an energy consumption of 0.210 kWh/m^3.

Key words | airlift reactor, desirability function, electrocoagulation/electro-flotation, response surface methodology (RSM), surface water

T. Ntambwe Kambuyi (corresponding author)
F. Eddaqaq
A. Driouich
B. Bejjany
H. Mellouk
K. Digua
A. Dani
Laboratory of Process Engineering and Environment, FST of Mohammedia, University Hassan II, Casablanca – Morocco, Hay Yasmina, B.P. 146, Mohammedia, 20650, Maroc
E-mail: *toussaint_ntambwe@yahoo.fr*

B. Lekhlif
Equipe de recherche Hydrogéologie, Traitement et Epuration des Eaux et Changements Climatiques, Ecole Hassania des Travaux Publics, Km 7, Route d'El Jadida, B.P. 8108, Oasis, Casablanca, Maroc

INTRODUCTION

Surface waters are used for the production of drinking water. However, the presence of many undesirable agents such as silts, clays, and algae causes them to become turbid and makes them unsuitable for human consumption. These particles have a small size ranging from 0.1 to 0.01 μm (Moussa *et al.* 2016; Naje *et al.* 2016) and remain suspended in water. Therefore, agglomeration of particles into a larger floc is a necessary step for their removal by flotation or sedimentation. A chemical coagulation/flocculation (CC/F) process is often used for destabilization and agglomeration of suspended particles by the addition of salts (i.e. alum). This method has some drawbacks like handling large quantities of chemicals, proper assessment of requirements, feeding of chemicals and production of a large volume of sludge causing a disposal problem and loss of water (Paul 1996). The regulations for drinking water, as well as for wastewater discharge, and new environmental considerations have allowed electrochemical technologies to gain an important place worldwide during the past two decades (Chen 2004). These technologies are characterized by low sludge production, and do not require the addition of chemical reagents.

doi: 10.2166/ws.2019.129

Electrocoagulation/electro-flotation (E_C/E_F) is an electrochemical technology which allows the generation of coagulants *in situ* by electrodissolution of a soluble anode. Metal ions (Al^{3+}, Fe^{2+} or Fe^{3+}) are generated at the anode while hydrogen gas bubbles are produced at the cathode. E_C/E_F has numerous advantages and some drawbacks as reported by many authors (Mouedhen *et al.* 2008; Zaroual *et al.* 2009; Khandegar & Saroha 2013). The electrode arrangement can be in a monopolar or bipolar mode (Kobya *et al.* 2011). Chemical reactions when aluminium is used as an electrode material are as follows:

- At the anode (oxidation of the metal):

$$Al_{(s)} \rightarrow Al^{3+}_{(aq)} + 3e^- \quad (1)$$

In the case of high anode potential, secondary reactions may occur (Hakizimana *et al.* 2017). This is the case of oxygen gas formation:

$$2H_2O \rightarrow O_2 + 4H^+ + 4e^- \quad (2)$$

- At the cathode:

$$2H_2O + 2e^- \rightarrow H_2 + 2OH^- \quad (3)$$

E_C/E_F efficiency is a function of three fundamental processes: electrochemical (electrolytic reactions at the surface of electrodes), coagulation (formation of coagulants in aqueous phase and adsorption of soluble or colloidal pollutants on coagulants), and flotation process (solid/liquid separation). The results of these processes and their interactions within the E_C/E_F reactor allow the removal of pollutants. However, their performance depends on some parameters such as pH, initial conductivity, treatment time, and applied voltage. To improve E_C/E_F efficiency, operating parameters have to be at their optimum values.

Most of the studies dealing with kinetics optimization make use of the traditional one-factor-at-a-time (OFAT) approach, examining the effect of one parameter on response, while holding all others constant. The result of this univariate analysis shows inadequate optimization towards response(s) (Sakkas *et al.* 2010). Indeed, the OFAT approach is time consuming, does not provide interaction effects and requires a large number of experiments (Zaroual *et al.* 2009). There is now increasing recognition that the OFAT approach is not efficient and ought to be replaced by soundly based chemometric methods such as response surface methodology (RSM) based on statistical design of experiments (DOEs). RSM is a multivariate analysis technic. It is based on the fit of a polynomial equation to the experimental data, which must describe the behaviour of a data set with the objective of making statistical previsions (Bezerra *et al.* 2008).

In this paper, a chemometric approach, especially RSM, is used to model and optimize turbidity removal efficiency (T_R) from surface water using the E_C/E_F process in an internal loop airlift reactor (ILAR) as a function of initial conductivity (X_1), applied voltage (X_2), treatment time (X_3), and inter-electrode distance (X_4).

MATERIALS AND METHODS

Preparation of the reconstituted solution

A reconstituted solution made by mixing clay particles and distilled water is used as a surface water. The clay particles are first ground and then sieved in order to remove particles exceeding 45 μm. Surface waters contain colloidal particles with a size ranging from 1 to 10^{-3} μm (Mickova 2015). In order to approach this characteristic, we study the sedimentation velocity of an isolated spherical particle in water (refer to Appendix A for the full survey results).

The reconstituted solution is characterized by an initial turbidity (T_i) of 107 NTU, which is the approximate turbidity value for surface waters (Bejjany *et al.* 2017), and pH = 7.3. The initial conductivity value is adjusted using sodium chloride (NaCl) as the electrolyte. An HI 99300 portable conductivity meter is used to measure the initial conductivity value. Turbidity is measured using a HACH series 2100 N brand turbidimeter. Tests are carried out in an ILAR with a volume capacity of 1 L. A sample of 850 mL from reconstituted solution is used for each test. Two flat aluminium electrodes are used in monopolar configuration and placed in a riser (refer to Appendix D) for the production of coagulants. T_R is given by:

$$T_R(\%) = \frac{T_i - T_f}{T_i} \times 100 \quad (4)$$

where T_i and T_f represent initial and final turbidity respectively.

The energy consumption (W_C) in electrocoagulation is calculated from:

$$W_C(\text{kWh/m}^3) = \frac{U}{V}\int_0^{t_e} I(t) \quad (5)$$

where U is the voltage applied (V), V the sample volume (m^3), t_e the treatment time (hours), and I the current (A).

Statistical analysis

Mathematical model

Central composite design (CCD) is used as a second-order response surface model in order to take into consideration extreme values. This design consists of three types of points: cube points that come from factorial design (2^k), axial points ($2k$) and central points (C_0). The central points are used to calculate experimental error (Sakkas *et al.* 2010). The experiment number is given by the following expression:

$$N = 2^k + 2k + C_0 \quad (6)$$

where k represents the number of factors.

Four factors are used in this study ($k = 4$). The experiment number can be divided into three groups as follows: $2^k = 2^4$ factorial experiments, $2k = 2*4$ axial experiments and $C_0 = 7$ central experiments (25–31, refer to Appendix C). Hence, 31 experiments are investigated in this study.

The second-order model can be expressed as follows:

$$Y = \beta_0 + \sum \beta_i X_i + \sum \beta_{ij} X_i X_j + \sum \beta_{ii} X_i^2 + \varepsilon \quad (7)$$

where Y is the theoretical response function, X_i, X_j represent the factors, β_0 is the constant term, and β_i, β_{ij}, β_{ii} represent respectively main (linear), interaction and quadratic effects coefficients. Table 1 shows the codification of real values (refer to Appendix B for full method calculations).

Optimization approach

The Derringer or desirability function is the most important and most current technique of optimization used when the optimal values for each response are located in different regions (Bezerra *et al.* 2008; Sakkas *et al.* 2010). The scale of the individual desirability function ranges from $d = 0$, for a completely undesirable response, to $d = 1$ for a fully desired response, above which other improvements would have no importance (Bezerra *et al.* 2008). The overall desirability is calculated as follows:

$$D = \sqrt[n]{d_1 d_2 \ldots d_n} \quad (8)$$

where n represents the number of responses to optimize and d_i the individual desirability.

RESULTS AND DISCUSSION

Preliminary experiments at the laboratory scale allowed factors to be highlighted which influence T_R from surface water by electrocoagulation/electro-flotation. The experimental domain is

Table 1 | Real and coded factors

			Factor coding				
Real factor (X_i)	**Units**	**Symbols**	**−2**	**−1**	**0**	**1**	**2**
Conductivity	(μS/cm)	X_1	250	725	1,200	1,675	2,150
Applied voltage	(V)	X_2	2	4	6	8	10
Treatment time	(min)	X_3	0.5	2.5	4.5	6.5	8.5
Inter-electrode distance	(mm)	X_4	6	10	14	18	22

as follows: 250–2,150 μS/cm, 2–10 V, 0.5–8.5 min, 6–22 mm, for X_1, X_2, X_3 and X_4 respectively.

Figure 1 shows the prediction profiler for T_R and W_C. The prediction profiler is often used to show how the prediction model changes as the settings of individual factors change. According to Figure 1, T_R and W_C increase with X_1, X_2 and X_3. On the other hand, when X_4 increases, T_R and W_C decrease.

Mouedhen *et al.* (2008) reported that the amount of Al^{3+} released in the aqueous solution is a function of the NaCl concentration of the electrolyte (conductivity). Indeed, the increase in X_1 leads to the breakdown of the anodic passive film. This allows the amount of Al^{3+} dissolved in the reactor to be increased, and therefore, suspended particles are quickly destabilized (Mouedhen *et al.* 2008). This result corresponds to those reported by Bejjany *et al.* (2017). In addition, the increase in X_1 during E_C/E_F is known to increase the production of hydrogen gas bubbles. In ILAR, electrodes are placed in a riser. Thus, hydrogen gas bubbles produced at the cathode are located in the riser. The increase in the amount of hydrogen gas bubbles leads to the creation of a density difference between the *riser* and *downcomer* ($\rho_{riser} < \rho_{downcomer}$), which allows recirculation movement. This phenomenon properly disperses Al^{3+} dissolved in the reactor and allows mixing of the suspension. Therefore, the collision of particles is promoted, which leads to the agglomeration of destabilized particles and their removal by flotation.

Applied voltage is a key parameter in E_C/E_F, which controls the amount of Al^{3+} dissolved, as well as hydrogen gas bubble production within the reactor (Bande *et al.* 2008). When X_2 increases, the amount of Al^{3+} dissolved, as well as the amount of hydrogen gas bubbles, increases in the reactor, which leads to the destabilization of suspended particles and their agglomeration.

T_R and W_C are strongly influenced by X_3. A longer X_3 leads to improved T_R and to increased W_C.

During the E_C/E_F process, a very fine film of metal hydroxides would get formed on, the anode, generating an extra resistance (Ghosh *et al.* 2008). The inter-electrode distance is one of the parameters on which this resistance (IR) strongly depends. The IR refers to the resistance of the media during the flow of electrical current through the cell. When X_4 increases, resistance to mass transfer becomes larger, therefore there is a smaller amount of Al^{3+} cations at the anode, leading to slower formation of coagulants in the middle (Ghosh *et al.* 2008). The rate of clay particle aggregation and adsorption of clays becomes lower, which explains the decrease in T_R. Nasrullah *et al.* (2012) and Khaled *et al.* (2015) report the same results.

W_C is defined as the electrical power consumed per unit volume. W_C is a function of X_1, X_2, X_3 and X_4 as shown in Figure 1. According to Figure 1, W_C increases with X_1, X_2 and X_3 as reported by Bejjany *et al.* (2017), Bazrafshan *et al.* (2014) and Zaroual *et al.* (2009), respectively. Inter-electrode distance has an opposite effect in comparison with other factors. Indeed, when X_4 increases, W_C decreases.

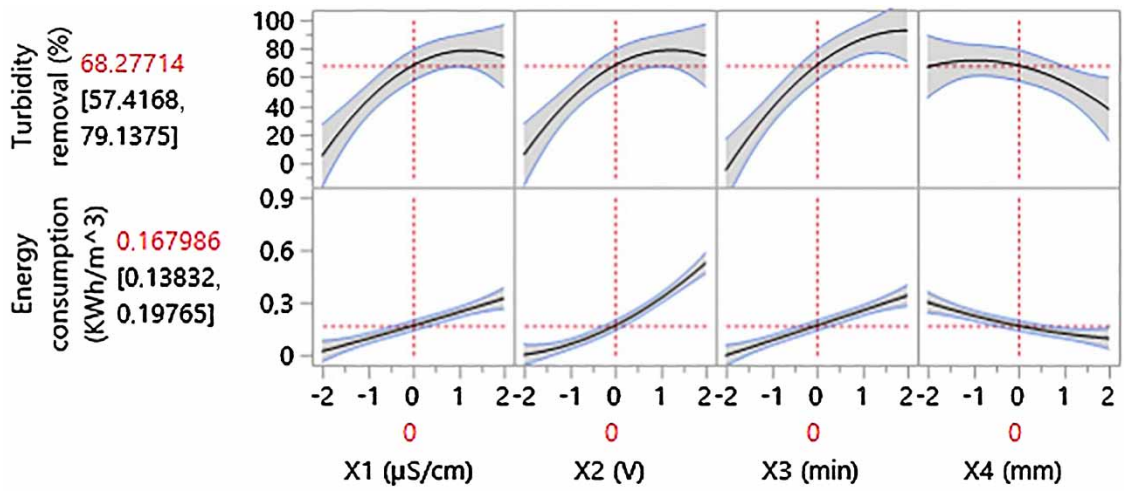

Figure 1 | Prediction profiler of T_R and W_C.

Table 2 shows experimental and predicted data for two responses. ANOVA is used to test the statistical significance of the ratio of mean square variation due to regression and mean square residual error. The *P*-value is used to estimate whether the F-ratio is large enough to indicate statistical significance. The model is statistically significant when the *P*-value is lower than 0.05 (Yi *et al.* 2010).

Table 2 | Experimental and predicted values for T_R and W_C

	T_R (%)		W_C (kWh/m^3)	
Standard Run	**Experimental values**	**Predicted values**	**Experimental values**	**Predicted values**
1	0	−4.229	0.0296	0.03216
2	0	−18.15	0.0174	0.08764
3	50.99	46.29	0.081	0.05749
4	11.98	29.15	0.0466	0.02024
5	0.99	21.43	0.142	0.13959
6	0	5.549	0.0831	0.04634
7	87.62	76.84	0.3754	0.40204
8	66.13	57.75	0.207	0.21607
9	12.94	23.72	0.0604	0.03779
10	0	14.77	0.0359	0.01624
11	72.64	71.08	0.1664	0.21014
12	76.96	58.92	0.08	0.09587
13	75.88	62.71	0.3327	0.36604
14	44.7	51.8	0.1858	0.19577
15	94.42	114.97	0.8593	0.77552
16	92.62	100.85	0.5081	0.51253
17	0	4.736	0.0347	0.02169
18	86.92	75.78	0.3042	0.32377
19	1.92	7.09	0.0113	0.00139
20	86.25	74.68	0.509	0.52547
21	2.88	−5.46	0.018	−0.00261
22	92.16	94.11	0.3123	0.33947
23	72.4	66.93	0.2923	0.30204
24	39.8	38.88	0.0977	0.09452
25	73.84	68.277	0.1783	0.167986
26	65.67	68.277	0.1613	0.167986
27	71.05	68.277	0.1647	0.167986
28	69.32	68.277	0.1743	0.167986
29	67.78	68.277	0.1669	0.167986
30	57.88	68.277	0.1658	0.167986
31	72.4	68.277	0.1646	0.167986

Figure 2 comes from linear regression between observed (experimental) and predicted values. It shows the fit of the predicted model to the experimental data. According to Figure 2, the *P*-values for the T_R and W_C regressions are lower than 0.05 (*P*-value < .0001). This result means that at least one of the terms in the regression equation has a significant correlation with the response variable. In conclusion, the form of model used in this study to explain the factors and response relationship is correct.

Furthermore, model precision is evaluated by a determination coefficient (R^2). The R^2 values for T_R and W_C are 0.92 and 0.98, respectively. These results imply that 92% and 98% of the sample variation for T_R and W_C, respectively, are attributed to the four factors. Only about 8% and 2% of the total variation for T_R and W_C, respectively, cannot be explained by the model. This indicates that the accuracy and general ability of the polynomial model are good.

The ANOVA table also provides a term for residual error, which measures the amount of variation in the response data left unexplained by the model. The root-mean-square error (RMSE) is 13.554 and 0.037 for the T_R and W_C model, respectively.

Unlike one-factor-at-a-time methodology, RSM also provides information about the interaction and quadratic effects of factors. This analysis is done by Fisher's F-test. In general, the smaller the value of *P*-values (<0.05), the larger the magnitude of the F-ratio, and the more significant is the corresponding coefficient term. The estimated regression coefficients, F-ratio and *P*-values for all the linear, quadratic and interaction effects of the parameters are given in Tables 3 and 4 for T_R and W_C, respectively. In Table 3, it is observed that the linear effect of X_1, X_2, X_3, and X_4, and the quadratic effect of X_1 (X_1^2), X_2 (X_2^2) and X_3 (X_3^2) are significant model terms. The corresponding *P*-value of all linear effects is <.0001, while the *P*-values of the quadratic effects are 0.0127, 0.0144 and 0.0287, respectively. All other model terms (all interaction effects and quadratic effect of X_4) can be said to be not significant (*P*-values > 0.05).

In addition, X_3 is the most significant model term with an F-ratio equal to 78.2564. The corresponding estimated coefficient value is 24.475. Based on the F-ratio values, the ranking of the significant model terms for T_R is as follows: $X_3 > X_1 > X_2 > X_1^2 > X_2^2 > X_4 > X_3^2$.

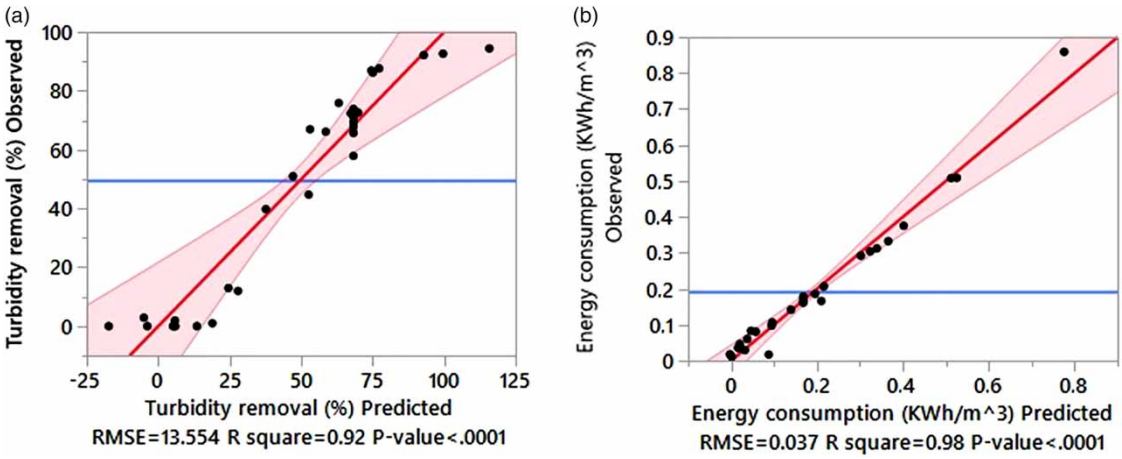

Figure 2 | Graphic model representation of (a) T_R and (b) W_C.

Table 3 | Estimated regression coefficients, F-ratio and *P*-values for T_R

Terms	Estimated coefficients	Degree of freedom	Sum of square	F-ratio	*P*-values
Constant	68.277	–	–	–	<.0001*
X_1	17.345	1	7,220.724	39.3033	<.0001*
X_2	17.313	1	7,193.69	39.1562	<.0001*
X_3	24.475	1	14,377.105	78.2564	<.0001*
X_4	−7.429	1	1,324.472	7.2093	0.0163*
X_1*X_2	3.957	1	250.51	1.3636	0.26
X_1*X_3	−1.413	1	31.951	0.1739	0.6822
X_1*X_4	0.618	1	6.113	0.0333	0.8575
X_2*X_3	1.849	1	54.723	0.2979	0.5928
X_2*X_4	0.136	1	0.294	0.0016	0.9686
X_3*X_4	−1.429	1	32.69	0.1779	0.6788
X_1^2	−7.108	1	1,444.903	7.8648	0.0127*
X_2^2	−6.952	1	1,382.08	7.5228	0.0144*
X_3^2	−6.093	1	1,061.728	5.7791	0.0287*
X_4^2	−3.948	1	445.792	2.4265	0.1389

*Significant model term (*P*-values <0.05).

In the same way, estimated regression coefficients, F-ratio and *P*-value results of W_C are indicated in Table 4. It shows that all linear effects of X_1, X_2, X_3 and X_4 are significant model terms (*P*-value < .0001). The two-level interaction effects of X_1*X_2, X_1*X_3, X_2*X_3, X_2*X_4 and X_3*X_4 are significant model terms. Their corresponding *P*-values are <.0001, 0.0011, <.0001, 0.0010 and 0.0235, respectively. Only the quadratic effect of X_2 (X_2^2) is a significant model term with a *P*-value = 0.0033. Thus, the two-level interaction effect of X_1*X_4 and the quadratic effects of X_1 (X_1^2), X_3 (X_3^2) and X_4 (X_4^2) are not significant model terms. Based on F-ratio values, X_2 is the most significant model term (F-ratio = 300.5864, estimated coefficient = 0.131). The ranking of significant model terms according to the F-ratio values for W_C is as follows: $X_2 > X_3 > X_1 > X_4 > X_2$*$X_3 > X_1$*$X_2 > X_2$*$X_4 > X_1$*$X_3 > X_2^2 > X_3$*$X_4$.

The regression model equations (second-order polynomial) relating T_R and W_C are developed and given in Equations (9) and (10), respectively. These equations only contain the significant model terms associated with their

Table 4 | Estimated regression coefficients, F-ratio and *P*-values for W_C

Terms	Estimated coefficient	Degree of freedom	Sum of square	F-ratio	*P*-values
Constant	0.1679	–	–	–	<.0001*
X_1	0.0755	1	0.13688151	99.8671	<.0001*
X_2	0.131	1	0.41199501	300.5864	<.0001*
X_3	0.0855	1	0.17553151	128.0656	<.0001*
X_4	−0.052	1	0.06459475	47.1275	<.0001*
X_1*X_2	0.0552	1	0.04876368	35.5774	<.0001*
X_1*X_3	0.0367	1	0.02161635	15.771	0.0011*
X_1*X_4	−0.0192	1	0.00593285	4.3285	0.0539
X_2*X_3	0.059	1	0.05622827	41.0234	<.0001*
X_2*X_4	−0.037	1	0.02211913	16.1378	0.0010*
X_3*X_4	−0.023	1	0.00859793	6.2729	0.0235*
X_1^2	0.0012	1	0.00004021	0.0293	0.8661
X_2^2	0.0238	1	0.01628072	11.8782	0.0033*
X_3^2	−0.00011	1	0.00000035	0.0003	0.9874
X_4^2	0.0075	1	0.00164013	1.1966	0.2902

*Significant model term (*P*-values <0.05).

estimated coefficients. The regression model equations are written as follows.

T_R model:

$$T_R = 68.277 + 17.345X_1 + 17.313X_2 + 24.475X_3 - 7.429X_4 - 7.108X_1^2 - 6.952X_2^2 - 6.093X_3^2 \quad (9)$$

W_C model:

$$W_C = 0.6179 + 0.0755X_1 + 0.131X_2 + 0.0855X_3 - 0.052X_4 + 0.0552X_1X_2 + 0.036X_1X_3 + 0.059X_2X_3 - 0.037X_2X_4 - 0.023X_3X_4 + 0.0238X_2^2 \quad (10)$$

Figures 3 and 4 show two-dimensional contour plots and three-dimensional response surface plots of T_R and W_C, respectively. These figures show interaction effects for two factors (the factors with most effect) when others are kept constant in their central values. These representations are often used to search optimal conditions of parameter process, especially when optimal values are located in the same region.

According to Figures 3 and 4, the optimum values of each response are located in different regions. For example, in Figure 3(a) (or Figure 4(a)), for a constant initial conductivity value (with $X_2 = 6$ V and $X_4 = 14$ mm), increase in treatment time leads to improvement in T_R. On the other hand, Figure 3(b) (or Figure 4(b)) shows that at a constant value of applied voltage, increase in treatment time leads to increase in W_C (with $X_1 = 1{,}200$ µS/cm and $X_4 = 14$ mm). Thus, changes in the level of a factor can improve one specific response and have a very negative effect on another one. Multicriteria methodology, especially the desirability function, is used to overcome this problem. Table 5 shows the scale of the individual desirability function for T_R and W_C. The scale of the individual desirability function ranges from $d = 0.01$, for a completely undesirable response (low T_R or high W_C) to $d = 0.98$, for a fully desired response (high T_R or low W_C). The overall desirability (D) close to 1 expressing the maximum of T_R and the minimum of the W_C is equal to 0.79. The optimum conditions relating to this value for each factor in coded values are 0.6046869 ($X_1 = 1{,}487$ µS/cm), −0.5 ($X_2 = 5$ V), 1 ($X_3 = 6.5$ min) and 0 ($X_4 = 14$ mm). The corresponding estimated values for T_R and W_C are 84.15% and 0.215 kWh/m^3, respectively. These values are used at the laboratory scale for the confirmation study as shown in Table 6.

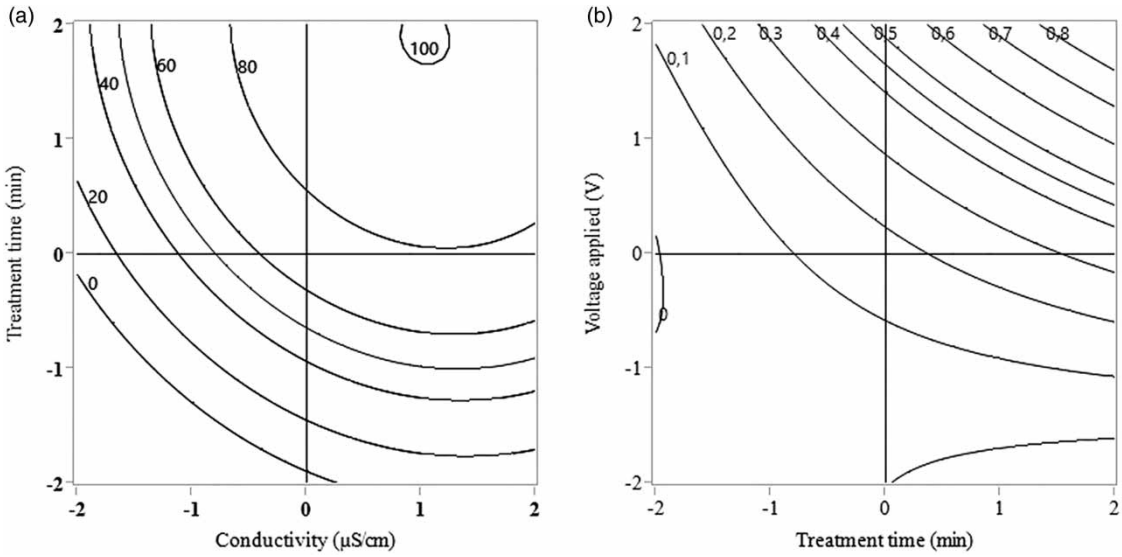

Figure 3 | 2D contour plot of (a) T_R ($X_2 = 6$ V and $X_4 = 14$ mm) and (b) W_C ($X_1 = 1{,}200$ µS/cm and $X_4 = 14$ mm).

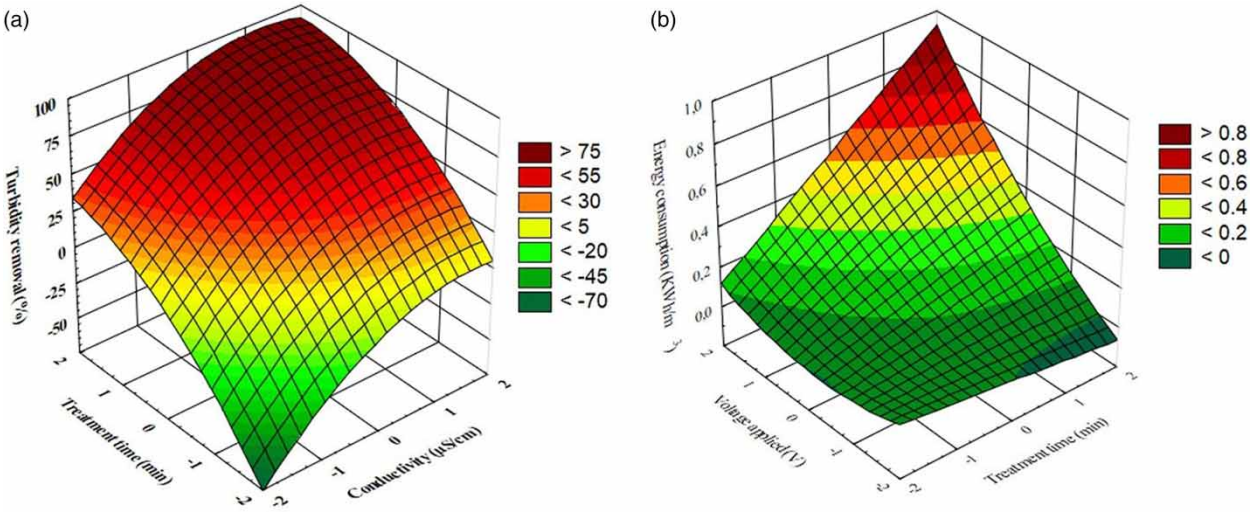

Figure 4 | 3D response surface plot of (a) T_R ($X_2 = 6$ V and $X_4 = 14$ mm) and (b) W_C ($X_1 = 1{,}200$ µS/cm and $X_4 = 14$ mm).

Table 5 | The scale of the individual desirability function for T_R and W_C

	T_R		W_C	
	T_R (%)	Desirability	W_C (KWh/m^3)	Desirability
High value	100	0.98	0.8	0.01
Mean value	50	0.5	0.45	0.5
Low value	0	0.01	0	0.98

Table 6 shows the results of the confirmation study. It shows that T_R and W_C under optimal conditions carried out at the laboratory scale are 72.05% and 0.210 kWh/m^3, respectively. The results found by Bejjany *et al.* (2017) for the same T_R value (72%) report a W_C of 0.357 kWh/m^3 under $X_1 = 351$ µS/cm, $X_2 = 12$ V, $X_3 = 7.5$ min and $X_4 = 18$ mm conditions. In comparison with our results, we

Table 6 | Optimum conditions for T_R by E_C/E_F in an ILAR

Factors	Units	Estimated values	Experimental values
X_1	μS/cm	1,487	1,500
X_2	V	5	5
X_3	min	6.5	6.5
X_4	mm	14	14
T_R	%	84.15	72.05
W_C	kWh/m^3	0.215	0.210

note that the RSM allowed us to obtain a W_C value of 41% less for the same T_R value.

CONCLUSION

In the present study, RSM is used in conjunction with CCD to optimize the removal of turbidity from surface water by E_C/E_F in an ILAR. The validation of the model is carried out by an appropriate analysis of variance (ANOVA). The results revealed that the model prediction used to explain factors and response relationship is correct with *P*-values <.0001. Furthermore, the determination coefficients of T_R and W_C are 0.92 and 0.98, respectively. Fisher's test is used to check the significance of all model terms on two responses. Therefore, corresponding regression equations are developed. These equations are used to build 3D response surface and 2D contour plots. These graphical representations allow the optimal conditions of parameter process to be searched. Since optimal values are located in different regions, a desirability function is used to allow the determination of optimal conditions for each response simultaneously. For the overall desirability function of 0.79, the optimal conditions are 1,487 μS/cm, 5 V, 6.5 min and 14 mm, respectively for X_1, X_2, X_3 and X_4. Under these conditions, the estimated T_R and W_C are 84.15% and 0.215 kWh/m^3, respectively. The confirmation study at the laboratory scale using optimal conditions shows 72.05% for T_R and 0.210 kWh/m^3 for W_C.

DISCLOSURE STATEMENT

The authors reported no potential conflict of interest.

REFERENCES

Bande, R. M., Prasad, B., Mishra, I. M. & Wasewar, K. L. 2008 Oil field effluent water treatment for safe disposal by electroflotation. *Chemical Engineering Journal* **137**, 503–509.

Bazrafshan, E., Mahvi, A. H. & Zazouli, M. A. 2014 Textile wastewater treatment by electrocoagulation process using aluminum electrodes. *Iranian Journal of Health Sciences* **2** (1), 16–29.

Bejjany, B., Lekhlif, B., Eddaqaq, F., Dani, A., Mellouk, H. & Digua, K. 2017 Treatment of the surface water by electrocoagulation–electroflotation process in internal loop airlift reactor: conductivity effect on turbidity removal and energy consumption. *Journal of Materials and Environmental Sciences* **8** (8), 2757–2768.

Bezerra, M. A., Santelli, R. S., Oliveira, E. P., Villar, L. S. & Escaleira, L. A. 2008 Response surface methodology (RSM) as a tool for optimization in analytical chemistry. *Talanta* **76** (5), 965–977.

Chen, G. 2004 Electrochemical technologies in wastewater treatment. *Separation and Purification Technology* **38** (1), 11–41.

Ghosh, D., Solanki, H. & Purkait, M. K. 2008 Removal of Fe(II) from tap water by electrocoagulation technique. *Journal of Hazardous Materials* **155**, 135–143.

Hakizimana, J., Gourich, B., Chafi, M., Stiriba, Y., Vial, C., Drogui, P. & Naja, J. 2017 Electrocoagulation process in water treatment: a review of electrocoagulation modeling approaches. *Desalination* **404**, 1–21.

Khaled, B., Wided, B., Béchir, H., Elimame, E., Mouna, L. & Zied, T. 2015 Investigation of electrocoagulation reactor design parameters effect on the removal of cadmium from synthetic and phosphate industrial wastewater. *Arabian Journal of Chemistry*. http://dx.doi.org/10.1016/j.arabjc.2014.12.012.

Khandegar, V. & Saroha, A. K. 2013 Electrocoagulation for the treatment of textile industry effluent: a review. *Journal of Environmental Management* **128**, 949–963.

Kobya, M., Ulu, F., Gebologlu, U., Demirbas, E. & Oncel, M. S. 2011 Treatment of potable water containing low concentration of arsenic with electrocoagulation: different connection modes and Fe–Al electrodes. *Separation and Purification Technology* **77** (3), 283–293.

Mickova, I. L. 2015 Advanced electrochemical technologies in wastewater treatment part I: electrocoagulation. *American Scientific Research Journal for Engineering, Technology, and Sciences* **14** (2), 233–257.

Mouedhen, G., Feki, M., De Petris Wery, M. & Ayedi, H. F. 2008 Behaviour of aluminum electrodes in electrocoagulation process. *Journal of Hazardous Materials* **150** (1), 124–135.

Moussa, D. T., El-Naas, M. H., Nasser, M. & Al-Marri, M. J. 2016 A comprehensive review of electrocoagulation for water treatment: potentials and challenges. *Journal of Environmental Management* **186** (1), 24–41.

Naje, A. S., Chelliapan, S., Zakaria, Z., Ajeel, M. A. & Alaba, P. A. 2016 A review of electrocoagulation technology for the treatment of textile wastewater. *Reviews in Chemical Engineering* **33** (3), 263–292.

Nasrullah, M., Singh, L. & Wahid, Z. A. 2012 Treatment of sewage by electrocoagulation and the effect of high current density. *Energy and Environmental Engineering Journal* **1** (1), 27–31.

Paul, A. B. 1996 Electrolytic treatment of turbid water in package plant. In: *22nd WEDC Conference*, pp. 286–288.

Sakkas, V. A., Azharul Islam, M., Stalikas, C. & Albanis, T. A. 2010 Photocatalytic degradation using design of experiments: a review and example of the Congo red degradation. *Journal of Hazardous Materials* **175**, 33–44.

Yi, S., Su, Y., Qi, B., Su, Z. & Wan, Y. 2010 Application of response surface methodology and central composite rotatable design in optimizing the preparation conditions of vinyltriethoxysilane modified silicalite/polydimethylsiloxane hybrid pervaporation membranes. *Separation and Purification Technology* **71** (2), 252–262.

Zaroual, Z., Chaair, H., Essadki, A. H., El Ass, K. & Azzi, M. 2009 Optimizing the removal of trivalent chromium by electrocoagulation using experimental design. *Chemical Engineering Journal* **148** (2–3), 488–495.

First received 20 March 2019; accepted in revised form 29 August 2019. Available online 12 September 2019